EuroIntervention 2013;9:148-156

Emerging technologies: polymer-free phospholipid encapsulated sirolimus nanocarriers for the controlled release of drug from a stent-plus-balloon or a stand-alone balloon catheter

Pedro A. Lemos[1], MD, PhD; Vasim Farooq[2], MBChB, MRCP; Celso K. Takimura[1], MD, PhD; Paulo S. Gutierrez[1], MD, PhD; Renu Virmani[3], MD; Frank Kolodgie[3], PhD; Uwe Christians[4], MD, PhD; Alexander Kharlamov[2], MD; Manish Doshi[5], PhD; Prakash Sojitra[5], PhD; Heleen M.M. van Beusekom[2], PhD; Patrick W. Serruys[2]*, MD, PhD

1. Department of Interventional Cardiology, University of São Paulo Medical School, São Paulo, Brazil; 2. Department of Interventional Cardiology, Erasmus University Medical Centre, Thoraxcenter, Rotterdam, The Netherlands; 3. CVPath Institute Inc., Gaithersburg, MD, USA; 4. Department of Anesthesiology, University of Colorado Denver, Aurora, CO, USA; 5. Concept Medical Research Private Limited & Envision Scientific Private Limited, Surat, India

KEYWORDS

- delivery systems
- drug-eluting balloon
- drug-eluting stent
- drug release profile
- nanoparticles

Abstract

Drug-eluting stents have proven to be effective in reducing the risk of late restenosis. In order to achieve a controlled and prolonged release of the antiproliferative agent, current drug-eluting stents utilise various biodegradable as well as non-erodible polymeric blends to coat the stent surface and to serve as drug carriers. The utilisation of polymeric compounds in current drug-eluting stents may eventually limit their performance as well as their clinical applicability due to the potential induction of undesirable local reactions. The development of alternative, polymer-free drug carriers has the potential to overcome some of the limitations of current drug-eluting stent formulations. Moreover, improvements in drug carriers may also result in an expansion of the technological possibilities for other intravascular drug delivery systems, such as metal-free or even implant-free solutions.

This article describes the structure and the preclinical validation profile of a novel phospholipid encapsulated sirolimus nanocarrier, used as a coating in two formulations: a coronary stent-plus-balloon system and a stand-alone balloon catheter. The nanoparticles provided a stable, even and homogenous coating to the devices in both formulations. Dose-finding studies allowed the most appropriate identification of the best nanoparticle structure associated with an extremely efficient transfer of drug to all layers of the vessel wall, achieving high tissue concentrations that persisted days after the application, with low systemic drug leaks.

**Corresponding author: Department of Interventional Cardiology, Erasmus Medical Centre, 's-Gravendijkwal 230, 3015 CE Rotterdam, The Netherlands. E-mail: p.w.j.c.serruys@erasmusmc.nl*

DOI: 10.4244/EIJV9I1A21

Introduction

Over the past decade, drug-eluting stents have proven to be an efficacious strategy to reduce the risk of late restenosis. Their principle of action is based on the concept of local delivery of antirestenotic drugs in which the stent itself serves as the platform for the release of the active agent. Accumulated evidence suggests that sustained tissue exposure to high local concentrations of the drug is a key factor in order to maximise the results[1,2]. In order to achieve a controlled and prolonged release of the antiproliferative agent, current drug-eluting stents utilise various biodegradable as well as non-erodible polymeric blends to coat the stent surface and to serve as drug carriers[3,4].

The utilisation of polymeric compounds in current drug-eluting stents generates some caveats which, at least in theory, may eventually limit their performance as well as their clinical applicability. Previous reports have suggested that the polymeric stent coatings may potentially induce undesirable local reactions. This is relevant, since the polymeric coating remains at the site of the implantation long after the release of the drug. Importantly, even for biodegradable polymers, the release of the drug is completed, by definition, before the dissolution of the carrier with a time lag ranging from days to months.

The development of alternative, polymer-free drug carriers has the potential to overcome some of the limitations of current drug-eluting stent formulations. Moreover, improvements in drug carriers may also result in an expansion of the technological possibilities for other intravascular drug-delivery systems, such as metal-free or even implant-free solutions.

The present article describes a new nanocarrier formulation of intracoronary delivery of drugs to the vessel wall, which is polymer-free and may be applied to stent-based as well as to stentless intravascular devices.

Nanotechnology for intravascular drug delivery – rationale and challenges for its development

The intact arterial wall poses a significant barrier to drug penetration[5]. Previous studies have indicated that the intimal and medial layers of elastic arteries are mostly impermeable to drug delivery, both in normal as well as in atherosclerotic vessels[5,6]. Conversely, drug tissue penetration is increased in regions with a solution of continuity, such as a dissection[5]. As a result, much of the drug load may remain unabsorbed, and strategies to increase local drug availability are critical to improve the efficiency of the system[7,8]. Particle size appears to affect cellular uptake, with smaller particles being more prone to cell internalisation[9,10]. In this regard, nano-sized particles (1 nanometer=10^{-3} micrometres=10^{-6} millimetres) may be particularly useful as the working unit for local vascular drug delivery.

Previous studies have shown that vascular exposure to antiproliferative drugs must be sustained over a period time for an adequate antirestenotic effect. Indeed, most, if not all, formulations of drug-eluting stents provide an initial burst of drug release which is followed by a sustained release plateau that lasts some weeks after implantation[1,2,11]. Currently, drug-eluting stents are coated with biostable or bioerodible polymeric blends that function as local reservoirs of the drug, which are slowly released until the carrier content is exhausted[3].

Conversely, nanocarriers offer an additional and different approach for increasing local bioavailability. Cellular uptake of nanoparticles is a rapid process[12], which may also occur actively, via endocytosis[13]. The endothelial coverage, which is the first and ultimate barrier for drug penetration in the arterial wall, has previously been shown to be responsive to nanoparticle uptake[12]. Both within the extracellular and intracellular compartments, nanoparticles may provide sustained release and prolonged drug effects, along with a protection against degradation for the encapsulated agent. In this regard, nanocarriers may be ideal carriers for rapamycin and other limus-like agents, particularly for implantless devices (e.g., drug-eluting balloons). This family of drugs tends to be unstable and they are not as lipophilic as other agents, such as paclitaxel. Therefore, sirolimus-based formulations behave suboptimally in such devices built on the principle of van der Waals forces (i.e., relating to the attractive or repulsive forces between molecules). Conversely, by encapsulating the drug in a protective packet, nanoparticle-based technology allows for the development of drug-delivery devices that work on Fick's law of diffusion and the concentration gradient of tissue, more appropriate for sirolimus-containing formulations.

However, size alone does not seem to be the sole factor governing particle uptake[6]. Previous studies have shown that the modification of the nanoparticle surface may markedly increase uptake and retention in the arterial wall[14]. Also, the concentration of particles in the infusate as well as the timing and pressure of exposure have been shown to be potential factors affecting final tissue penetration[15,16].

The drug carrier described here was optimised for intravascular application and was developed based on the premises above. Its development aimed for a nano-sized drug-containing particle that was fully degradable and polymer-free, with enhanced uptake properties at tissue level. Furthermore, it had to be capable of containing and being loaded with a significant quantity of limus-based drugs and providing a uniform coating to the surface of the device, whilst being resistant to sterilisation and mechanical forces.

Description of the novel nanocarrier coating and derived drug-delivery devices

The basic unit for the novel carrier is a phospholipid bilayer nanoparticle which encapsulates sirolimus **(Figure 1)**. Its envelope is made up of a lipid-based component with a hydrophilic head and two lipophilic tails, with the addition of a calcium phosphorus-based component sparsely located at the particle membrane. The latter component, which comprises approximately 5% of the particle mass, is sensitive to subtle variations in pH and controls the release of the drug content.

Manufacturing process of nanoparticles

The nanoparticles were synthesised using an ultrasonic homogeniser. In brief, 50 mg of sirolimus was dispersed in 25 ml of HPLC grade water (Rankem-RFCL Ltd, Faridabad, India) containing 1%

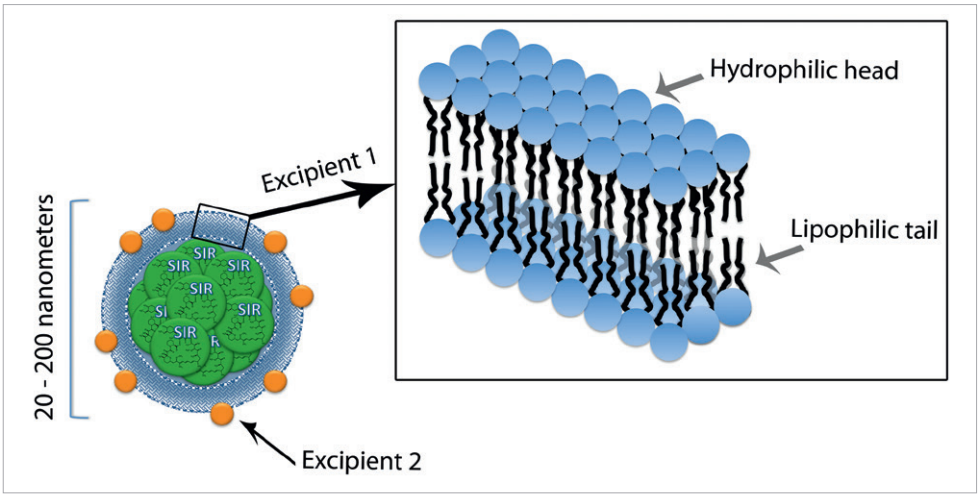

Figure 1. *Schematic illustration of the ultrastructure of the nanoparticle containing sirolimus (nucleus, in green), incorporating the combination of two excipient carriers to allow penetration and release of the active agent. Excipient 1 is a lipid-based component with a hydrophilic head and two lipophilic tails, which is the basic unit of a bilayer membrane that encapsulates the particle (note the detail in the right upper panel). Excipient 2 is integrated in the particle envelope, comprising ~5% of the coating mass. It is a calcium-phosphorus-based component with enhanced haemocompatibility that is readily absorbed into the vessel wall and releases the encapsulated drug on variation in pH.*

Tween 80 and 0.01% Mannitol (both by Sigma-Aldrich, St. Louis, MO, USA). The aqueous solution of sirolimus (25 ml) was subjected to ultrasonic homogenisation using a customised machine for 10 to 20 minutes in an ice-cold water bath to obtain sirolimus nanocrystals. The sirolimus nanocrystals were subsequently encapsulated using an aqueous solution of Lipoid E80 (Lipoid GmbH, Ludwigshafen, Germany). The solution was analysed for particle size detection using the Malvern Zetasizer (ZS90) (Malvern Instruments Ltd, Malvern, UK) size detector **(Figure 2)**, which showed Z average particle size of 210 nm, with a Zeta potential of the formulation of –33.2 mV, indicating a moderately stable aqueous formulation.

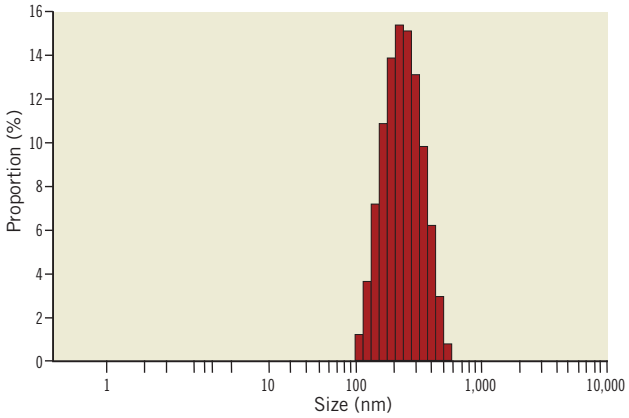

Figure 2. *Histogram of size distribution of the sirolimus nanocarrier.*

Coating process of sirolimus nanoparticles to a metallic stent platform and balloon-catheter delivery system, and to a stand-alone balloon catheter

The sirolimus nanocarrier was used to coat two drug-delivery formulations: 1) a metallic stent already mounted in a balloon delivery system, and 2) a stand-alone balloon catheter. Both formulations were coated using an inert gas assisted spray process. For the drug-eluting stent formulation, the nanoparticle carrier was applied in stents already crimped onto the balloon delivery system. Consequently, the coating was uniformly distributed over the stent-plus-balloon surface, with only the abluminal face of the stent struts having the coating applied **(Figure 3)**. The coated stent-plus-balloon and stand-alone balloon catheter were analysed by scanning electron micrography (SEM) to evaluate surface smoothness and coating defects. The surfaces of the coated devices were smooth, without irregularities, cracks, or flakes **(Figure 3)**. The drug content of the nanocarrier sirolimus-eluting stent-plus-balloon (108 µg of drug on a 3.0×16 mm stent), and the nanocarrier stand-alone sirolimus-eluting balloon (180 µg of drug on a 3.0×15 mm balloon), was comparable to the drug load of the commercially available Cypher™ (Cordis, Johnson & Johnson, Warren, NJ, USA) sirolimus-eluting stent (153 µg of drug on a 3.0×18 mm stent). Specifications of both nanocarrier-based formulations are presented in **Table 1**.

In vitro and *in vivo* drug release behaviour

IN VITRO DRUG RELEASE PROFILE

In vitro drug release was analysed using HPLC, in PBS 7.4, at different intervals up to 40 days. HPLC operating parameters were selected as: flow rate 1.0 ml/min. (±0.01); λ maxima 277 nm (±1 nm); column temperature 50°C (±2°C); sensitivity of detector 0.02 AUFS; injection volume 20 µL; analysis time 20 minutes.

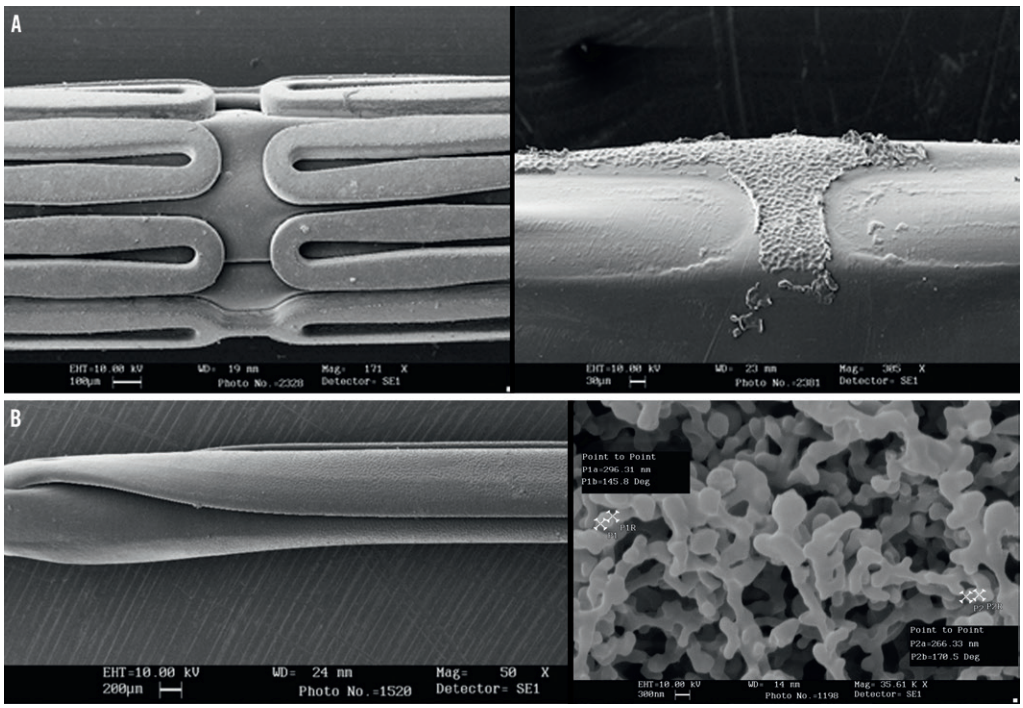

Figure 3. *A) Scanning electron micrography of the nanocarrier drug-eluting stent formulation. From left to right: pre-crimped coated stent; balloon after removal of stent. B) Scanning electron micrography of the nanocarrier drug-eluting balloon formulation (left panel). Right panel: high magnification microphotography of the nanocarrier coating.*

Table 1. Specifications of nanocarrier sirolimus-eluting stent and nanocarrier sirolimus-eluting balloon.

Nanocarrier sirolimus-eluting stent	
Delivery system	Same as for the nanocarrier sirolimus-eluting balloon (see below)
Metallic alloy	Cobalt-chromium L-605
Strut thickness	73 µm
Nanocarrier sirolimus-eluting balloon	
Catheter material	Polyamide
Balloon material	COPAN Co-Polyamide
Tip profile	0.016"
Tip design	Soft stepless tip
Hypotube diameter	1.7 Fr
Shaft coating	Hydraflow® hydrophilic coating
Nominal pressure	6 atm
Avg. burst pressure	25 atm
Drug coating	Encapsulated nanoparticle of sirolimus
Drug load	180 µg of sirolimus on a 3.0×15 mm balloon

Mobile phase included acetonitrile:methanol:water in a concentration ratio of 22:67:11. Mobile phase was subsequently degassed in an ultrasonic cleaner for 10 minutes. As shown in **Figure 4**, the release chart clearly indicated that sirolimus was delivered from the stents with an initial burst followed by a sustained release for up to 40 days.

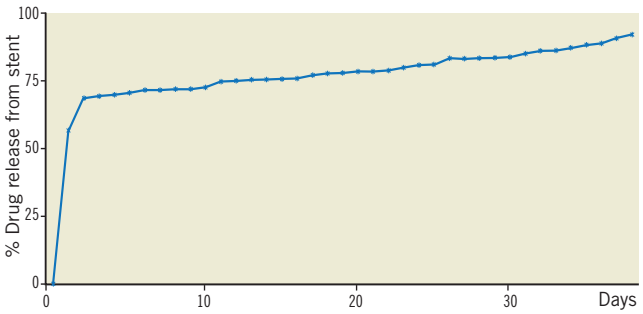

Figure 4. *In vitro release of sirolimus from nanoparticle-coated stents.*

IN VIVO DRUG RELEASE PROFILE

Local and systemic drug release was evaluated *in vivo* for the nanocarrier sirolimus-eluting balloon. Experiments were performed in a total of nine New Zealand white male rabbits, five to six months old, 3.0-4.0 kg. Through the left common carotid artery, under fluoroscopy, both iliofemoral arteries were injured by endothelial denudation with a 3 Fr Fogarty embolectomy catheter. Immediately after the arterial balloon denudation, also under fluoroscopy, a drug-eluting balloon was inflated for 60 seconds (7 atm) in both iliac arteries. Immediately after the drug-eluting balloon inflation, bilateral bare metal stents were implanted in each iliac artery over the same site, under fluoroscopy. Whole blood was collected from the central ear artery for serum drug analysis at 30 min, one hour, three hours, and 24 hours post implant.

The animals were euthanised at one, eight, and 14 days (390 mg sodium pentobarbital and 50 mg phenytoin sodium) and tissue around the stent was dissected free, weighed, and snap-frozen in liquid nitrogen for drug measurement by HPLC tandem mass spectrometry.

Figure 5 illustrates the blood concentration and the tissue concentration of sirolimus over time, after a single 60-second inflation of the nanocarrier sirolimus-eluting balloon. The blood concentration was higher 30 min after balloon inflation (9.3 ng/ml) and rapidly decreased to 0.8 ng/ml at 24 hours **(Figure 5)**. Although the tissue concentration of sirolimus also peaked acutely (140.6 ng/mg at the first day), the drug was still detectable in the tissue two weeks after the index procedure (5.5 ng/mg at 14 days) **(Figure 5)**.

When contrasted against previous results after implantation of two overlapped Cypher™ (Cordis) sirolimus-eluting stents in a similar experimental model[17], the nanocarrier sirolimus-eluting balloon seemed to produce lower blood concentrations (at 30 min: balloon 9.3 ng/ml and Cypher™ 13.3 ng/ml; at 24 hours: balloon 0.8 ng/ml and Cypher™ 4.6 ng/ml) and a higher release of sirolimus to the tissue (at one day: balloon 140.6 ng/mg and Cypher™ 4.5 ng/mg; at eight days: balloon 15.5 ng/mg and Cypher™ 1.6 ng/mg). These findings suggest the efficiency of the new technology to deliver sirolimus locally to the vessel wall tissue. It must be acknowledged, however, that these pharmacokinetic results only apply to the situation where a stent is implanted before the sirolimus-balloon inflation and should not be directly extrapolated to the context of isolate sirolimus-eluting balloon use.

IN VIVO TEMPORAL VESSEL WALL DISTRIBUTION

The study aimed to evaluate the vessel wall distribution of DTF-labelled (5-[4,6-dichlorotriazinyl]aminofluorescein) sirolimus nanoparticles in rabbits, after one hour, 24 hours, three days and seven days from inflation of a nanoparticle sirolimus-eluting balloon. Iliofemoral arteries (n=four animals; eight arteries) were treated bilaterally with DTF-labelled nanoparticle sirolimus (a description of the experimental model is provided in the section above). No stent was implanted after the balloon inflation. The samples were harvested and imaged longitudinally *en face* and in histologic cryosections (cross-sections) by confocal microscopy.

To determine the extent and distribution of nanoparticle sirolimus on the luminal surface, the iliofemoral arteries were opened longitudinally and positioned face down on a histologic slide in aqueous mounting media. The DTF-labelled nanoparticle sirolimus adherent to the luminal surface of the artery were viewed *en face* using a Zeiss Pascal confocal microscope, equipped with a 488-nm excitation argon laser (green channel) where images were acquired under a 40x oil immersion objective. The depth and circumferential distribution of DTF-labelled sirolimus nanoparticles were examined in histological sections prepared in cross-section. For these studies, 2-3-mm unfixed artery segments were snap-frozen in liquid nitrogen cooled isopentane for serial cross-sections cut at 10 µm, using a standard cryostat (Thermo Shandon Cryotome®; Thermo Fisher Scientific, Waltham, MA, USA). Histological sections were mounted on glass slides and also viewed by confocal microscopy.

After one hour, the DTF-labelled nanoparticles were mostly confined to the luminal surface, involving approximately 60% to 70% of the circumferential area. Virtually no DTF signal was seen below the level of the internal elastic lamina **(Figure 6)**. After 24 hours, DTF-labelled sirolimus nanoparticles were primarily localised to the luminal surface involving approximately 30% to 40% of the circumferential area. Overall, in the first day, the majority of the DTF signal was observed at or below the internal elastic lamina.

After three days, DTF-labelled nanoparticles were observed on the luminal surface involving approximately 30% to 40% of the circumferential area. The majority of DTF signals were seen below the internal elastic lamina limits, with some positive signals deeper within the medial region **(Figure 6)**.

After seven days, histological sections showed the DTF label near the luminal surface involving approximately 30% to 40% of the circumferential area. The DTF signal was primarily observed in the medial layer, with the majority of the signals deep within the media, but with rare extensions into the adventitial layer **(Figure 6)**.

These findings strongly suggest that the nanoparticle sirolimus-eluting balloon is able to deliver the drug to the vessel. The drug remains retained at the delivery site for days after the inflation, migrating from the lumen surface to the deeper structures of the vessel wall itself. It is important to recognise, however, that the

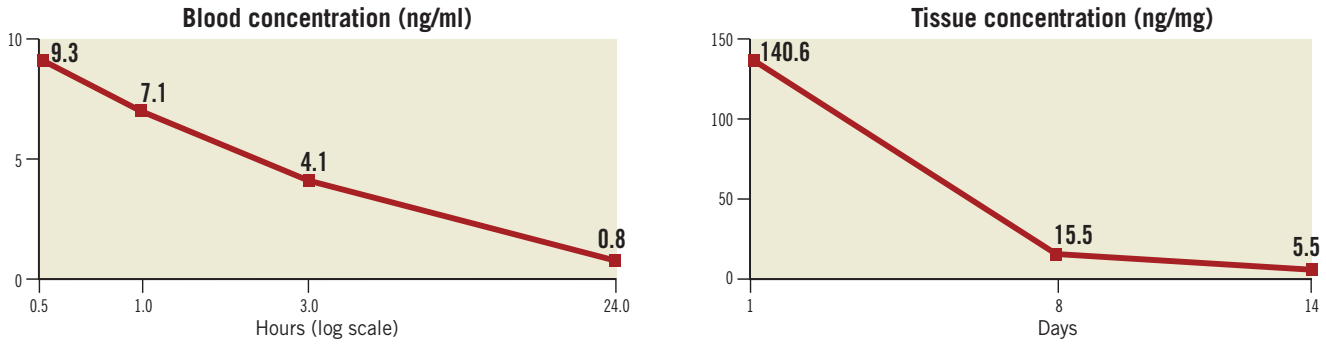

Figure 5. *Blood concentration (left) and tissue concentration (right) of sirolimus after a single 60-second inflation of the nanocarrier sirolimus-eluting balloon.*

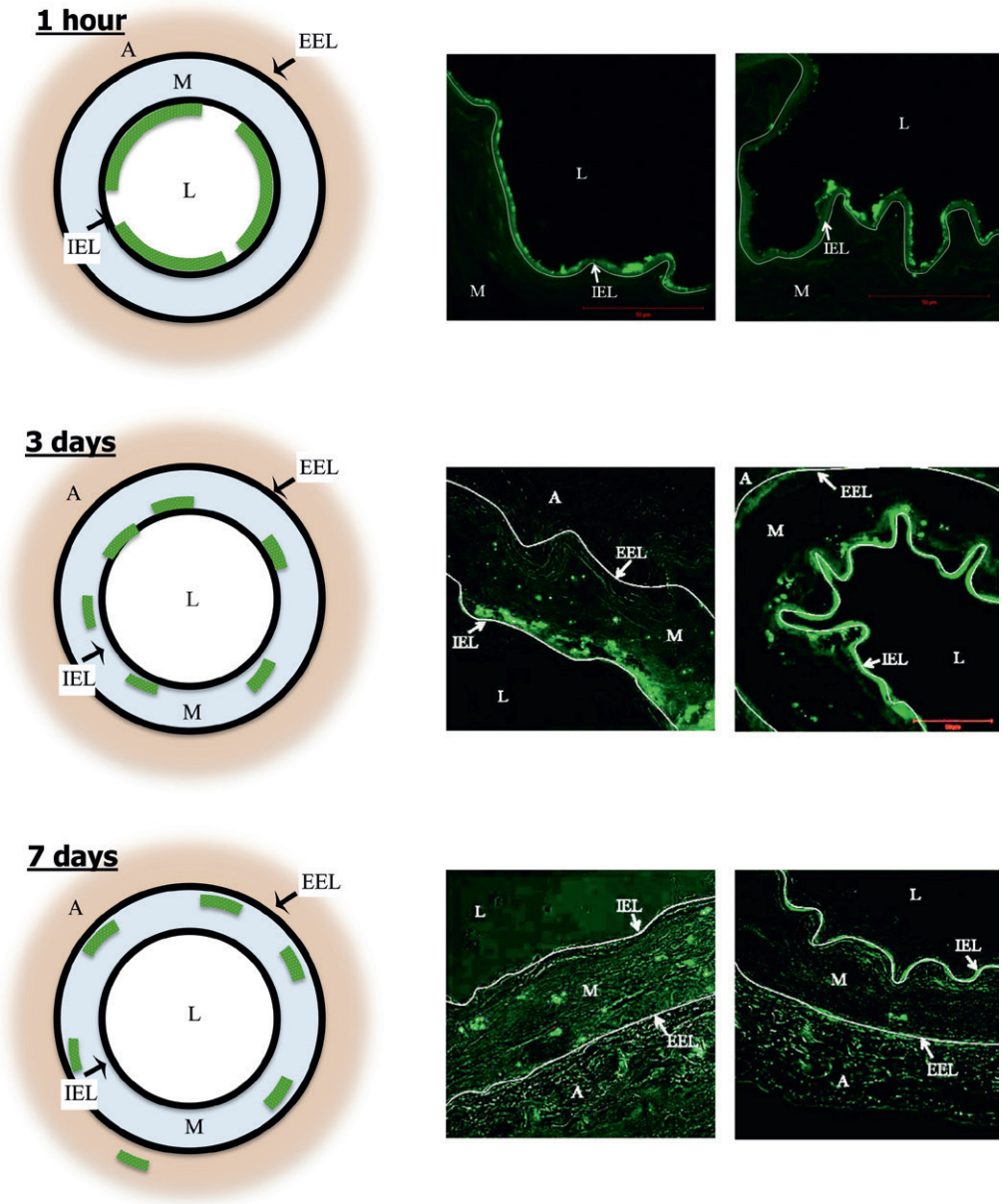

Figure 6. *Temporal penetration of DTF-labelled sirolimus nanoparticles after drug-eluting balloon inflation, as assessed by confocal microscopy. The left panels show a diagrammatic representation and the mid and right panels the actual cross-sectional images. At 1 hour (upper panels), 60% to 70% of circumferential area was marked with DTF signal. No particle was seen below the internal elastic lamina. At 3 days (mid panels), 30% to 40% of circumferential area presented DTF signal. The majority of particles were below the internal elastic lamina (some positive signals deeper in media). At 7 days (lower panels), 30% to 40% of circumferential area had DTF signal. Particles primarily in deep media, with rare extension into adventitia. A: adventitia; EEL: external elastic lamina; IEL: internal elastic lamina; L: lumen; M: media*

findings above were obtained in an experimental condition where a fluorescent probe was added to the molecule of sirolimus. Even though the additional radical is a largely used biological stain and is not expected significantly to disturb the pH or the lipophilicity of sirolimus, nor the size or the stability of the nanoparticles, critical features that basically modulate the bioavailability and the distribution of the drug, one cannot rule out minor changes in the properties of the drug and of the nanoparticle.

Pre-clinical assessment of safety and efficacy

DOSE-FINDING EVALUATION OF THE NANOPARTICLE/DRUG COMPONENTS

The effectiveness of the study nanoparticle to deliver a high concentration of sirolimus to the tissue is believed to be related to its chemical structure, mostly as a function of the calcium phosphorus-based excipient located at the envelope of the particle **(Figure 1)**. This study was conducted with the main objective of assessing

whether variations in the dose of the excipient would result in a difference in the biological effects of the nanoparticle.

The experiments were performed in a group of 14 juvenile domestic pigs, weighing approximately 18-23 kg. Under general anaesthesia, vascular access was obtained through the common femoral artery or common carotid artery after blunt dissection. Under fluoroscopy, after intravenous heparin, a guiding catheter was manipulated to the ascending aorta for the selective cannulation of both coronary arteries. Baseline angiograms of the right and left coronary arteries were obtained after intracoronary nitrate administration. Through a 0.014"guidewire, a bare metal stent was implanted at the right coronary artery, the left anterior descending artery, and the left circumflex artery in a non-tapered, non-bifurcation, non-angulated segment (i.e., three stents per animal). Stent sizes were selected to induce moderate vessel injury, with a stent:artery ratio of 1.1:1.0. Immediately after stent implantation, the stented site was post-dilated for 60 seconds (single inflation) with an additional balloon according to the following randomised groups:

1. Nanoparticle-coated balloon with excipient:drug ratio=1:1
2. Nanoparticle-coated balloon with excipient:drug ratio=0.5:1
3. Nanoparticle-coated balloon with excipient:drug ratio=0.25:1
4. Nanoparticle-coated balloon with excipient:drug ratio=1:0
5. Uncoated balloon

All animals were kept on aspirin and clopidogrel for 28 days, when a follow-up study was performed. Optical coherence tomography (OCT) imaging (M2 system; LightLab Imaging, Westford, MA, USA) of the target segments was performed during occlusion of the proximal coronary artery with a 4 Fr occlusion balloon catheter (Helios; LightLab Imaging), and saline flushing with a 0.016-inch OCT catheter (Image Wire; LightLab Imaging) at an automatic pullback speed of 1 or 2 mm/sec. During off-line OCT analyses, the lumen and stent boundaries were traced semi-automatically. The OCT neointimal area was calculated as the stent edge area minus lumen area and the percent neointimal obstruction was calculated as the neointimal area divided by the stent area, multiplied by 100.

After image acquisition the animals were euthanised, and the heart excised for immediate perfusion fixed with formalin (~80 mmHg). The target arteries and the tissue around the stents were dissected free and included in methacrylate resin. A total of three cross-sections (proximal, mid and distal) were obtained from each vessel on a rotary microtome (cut thickness 3 to 6 µm) and stained with haematoxylin and eosin and Verhoeff stains. For each cross-section, the degree of arterial injury at the site of stent struts was graded according to the methods proposed by Schwartz et al[18,19] and Gunn et al[20], and the degree of fibrin deposition and of inflammation were semi-quantitatively scored. The light microscopy neointimal area was calculated as the internal elastic lamina area minus lumen area, and the percent neointimal obstruction was calculated as the neointimal area divided by the internal elastic lamina area, multiplied by 100.

As shown in **Figure 7**, the nanoparticle sirolimus-eluting balloon with the highest excipient dosage (i.e., excipient:drug ratio=1:1) provided the largest inhibition of neointimal proliferation at 28 days, both by OCT and by light microscopy analyses. Furthermore, the inhibition of neointimal growth after the application of the high-dose excipient nanoparticle sirolimus-eluting balloon did not result in any significant inflammation or fibrin deposition **(Table 2)**.

Table 2. Bare metal stent implantation followed by study balloon inflation (see text for details of subgroups): morphological analysis by light microscopy after 28 days.

	Excipient drug ratio				
	0.25:1 (n=7)	0.5:1 (n=7)	1:1 (n=7)	1:0 (n=7)	POBA (n=7)
Inflammation score	1 (1-1)	1 (1-1)	1 (0-1)	1 (1-1)	1 (1-1)
Fibrin score	1 (0-1)	1 (0.5-1)	1 (0-1)	0 (0-0.5)	0 (0-1)
Schwartz injury score	1 (0.5-1)	1 (1-2)	1 (0.5-2)	1 (1.5-2)	1 (0.5-1)
Gunn injury score	2 (2-2)	2 (1.5-3)	1.5 (1.5-2)	2 (1-2.5)	1.5 (1.5-2)

Numbers are median (interquartile range); p<0.05 for all comparisons; POBA: plain old balloon angioplasty

Safety and efficacy in porcine and rabbit models

As described in the earlier section "Dose-finding evaluation of the nanoparticle/drug components", the sirolimus-eluting balloon was shown to inhibit neointimal proliferation effectively in a 28-day porcine model, in a protocol where it was locally applied after bare metal stent implantation.

The effects of the nanoparticle sirolimus-eluting balloon inflated before stent deployment were investigated in a separate experiment with eight rabbits. The animals were instrumented as detailed in the section "*in vivo* drug release profile" above. After endothelial denudation, the nanoparticle sirolimus-eluting balloon was inflated in one iliac artery and a control uncoated balloon was inflated in the contralateral iliac artery. Subsequently, a bare metal stent was implanted at the site where the study balloon was inflated. After 28 days, the animals were euthanised and the specimens analysed by light microscopy. Neointimal proliferation was very low and similar for both the nanoparticle-sirolimus balloon and the uncoated balloon groups (percent neointima obstruction: 11.48±1.30% vs. 11.49±1.49%, respectively, p>0.99; neointimal thickness: 0.030±0.0076 mm vs. 0.032±0.0098 mm, respectively, p=0.65). The neointima was composed primarily of smooth muscle cells and proteoglycans and rarely of fibrin; the re-endothelialisation was essentially complete for both groups. Overall, mean injury scores were low and similar between both groups (0.61 vs. 0.84, respectively, p=0.07). Intimal inflammation scores were low (control=0.58±0.24) to mild (nanoparticle sirolimus-eluting balloon=0.92±0.39), with a tendency to be more evident in the drug-eluting balloon group (p=0.05).

Summary and conclusions

This article describes the structure and the preclinical validation profile of a novel phospholipid encapsulated sirolimus nanocarrier,

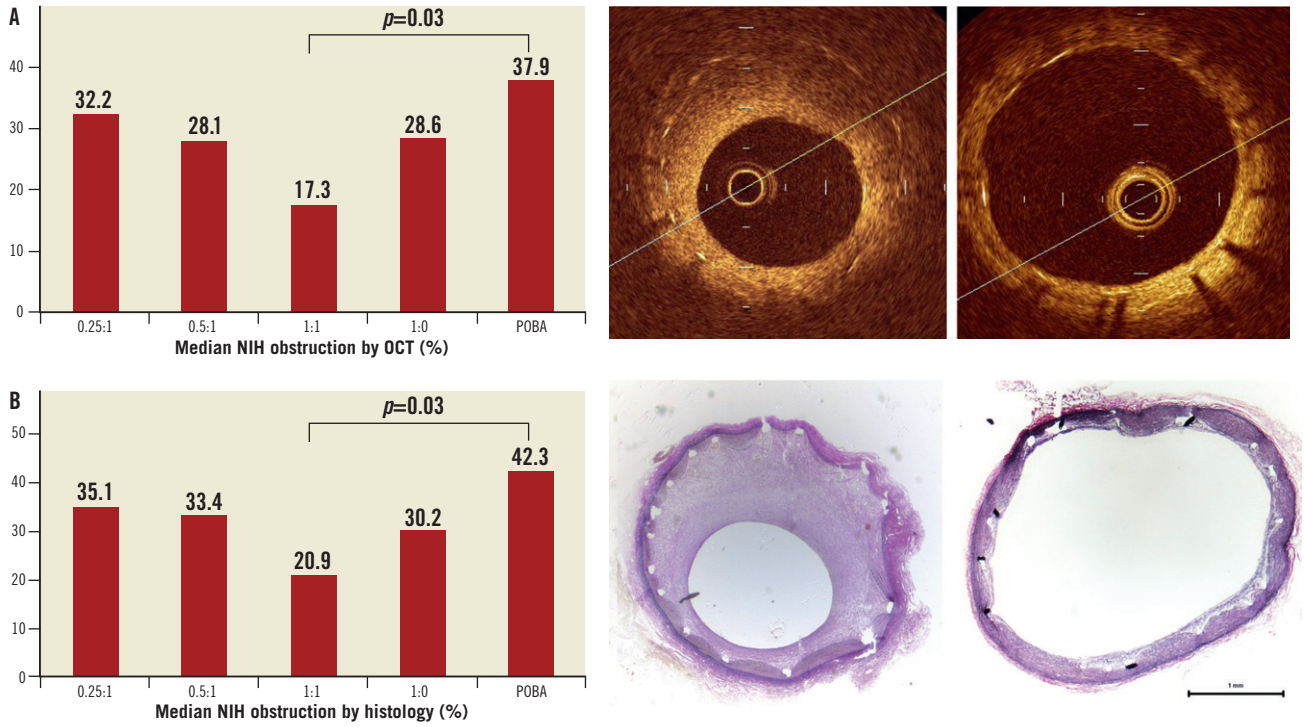

Figure 7. *Bare metal stent implantation followed by nanocarrier-sirolimus-coated balloon inflation (see text for details of subgroups). The graphs show the median neointimal percent obstruction across all study groups at 28 days, by OCT (upper left panel) and by light microscopy (lower left panels). The right panels illustrate OCT (upper) and light microscopy (lower) images of the group 1:1 excipient:drug ratio. For comparison, the mid panels demonstrate representative OCT (upper) and light microscopy (lower) images of the plain uncoated balloon group. NIH: neointima hyperplasia; POBA: plain old balloon angioplasty*

used as a coating in two formulations: a coronary stent-plus-balloon system and a stand-alone balloon catheter. The nanoparticles provided a stable, even and homogenous coating to the devices in both formulations. Dose-finding studies allowed the most appropriate identification of the best nanoparticle structure associated with an extremely efficient transfer of drug to all layers of the vessel wall, achieving high tissue concentrations that persisted days after the application, with low systemic drug leaks.

To the best of our knowledge, this is the first coating shown to be able to deliver sirolimus from a stentless formulation (i.e., drug-eluting balloon) efficiently. The new sirolimus-containing nanocarrier was shown to reduce neointimal proliferation, whilst maintaining a good safety profile in animal experimentation. The sum of these results warrants further investigation and indicates that this technology is a promising candidate for future clinical use. A first-in-man clinical study is currently on-going to evaluate the safety and feasibility in practice of drug-delivery devices with the novel nanocarrier.

Addendum

We opted to investigate the preclinical behaviour of this new technology in a comprehensive way, evaluating several parameters of post-procedure vascular healing in both porcine and rabbit models, which are generally used in similar validation studies worldwide[21]. Additionally, the studies directed to assess drug kinetics (both for imaging-based as well as chemical-analytic essays) were deliberately restricted to experiments with rabbits because this model has been more widely used in this scenario, potentially allowing for an indirect comparison with historical results from other technologies.

Conflict of interest statement

P. Lemos, C. Takimura and P. Gutierrez received institutional research grants from Concept Medical Research. R. Virmani is a consultant for Abbott Vascular, 480/Medical Arsenal Medical, Atrium Medical Corporation, Biosensors International, GlaxoSmithKline, CBard/Lutonix, Medtronic AVE, Terumo, W.L. Gore. M. Doshi is owner and P. Sojitra is employee of Concept Medical Research Pvt. Ltd & Envision Scientific Pvt. Ltd. H. van Beusekom has research contracts with Envision Ltd. The other authors have no conflicts of interest to declare.

References

1. Serruys PW, Sianos G, Abizaid A, Aoki J, den Heijer P, Bonnier H, Smits P, McClean D, Verheye S, Belardi J, Condado J, Pieper M, Gambone L, Bressers M, Symons J, Sousa E, Litvack F. The effect of variable dose and release kinetics on neointimal hyperplasia using a novel paclitaxel-eluting stent platform: the Paclitaxel In-Stent Controlled Elution Study (PISCES). *J Am Coll Cardiol.* 2005;46:253-60.

2. Farooq V, Gogas BD, Serruys PW. Restenosis: delineating the numerous causes of drug-eluting stent restenosis. *Circ Cardiovasc Interv.* 2011;4:195-205.

3. Garg S, Serruys PW. Coronary stents: looking forward. *J Am Coll Cardiol.* 2010;56:S43-78.

4. Lemos PA, Moulin B, Perin MA, Oliveira LA, Arruda JA, Lima VC, Lima AA, Caramori PR, Medeiros CR, Barbosa MR, Brito FS Jr, Ribeiro EE, Martinez EE; PAINT trial investigators. Randomized evaluation of two drug-eluting stents with identical metallic platform and biodegradable polymer but different agents (paclitaxel or sirolimus) compared against bare stents: 1-year results of the PAINT trial. *Catheter Cardiovasc Interv.* 2009;74:665-73.

5. Rome JJ, Shayani V, Flugelman MY, Newman KD, Farb A, Virmani R, Dichek DA. Anatomic barriers influence the distribution of *in vivo* gene transfer into the arterial wall. Modeling with microscopic tracer particles and verification with a recombinant adenoviral vector. *Arterioscler Thromb.* 1994;14:148-61.

6. Nasser TK, Wilensky RL, Mehdi K, March KL. Microparticle deposition in periarterial microvasculature and intramural dissections after porous balloon delivery into atherosclerotic vessels: quantitation and localization by confocal scanning laser microscopy. *Am Heart J.* 1996;131:892-8.

7. Kutryk MJ, Foley DP, van den Brand M, Hamburger JN, van der Giessen WJ, deFeyter PJ, Bruining N, Sabate M, Serruys PW; ITALICS Trial. Local intracoronary administration of antisense oligonucleotide against c-myc for the prevention of in-stent restenosis: results of the randomized investigation by the Thoraxcenter of antisense DNA using local delivery and IVUS after coronary stenting (ITALICS) trial. *J Am Coll Cardiol.* 2002;39:281-7.

8. Camenzind E, Bakker WH, Reijs A, van Geijlswijk IM, Boersma E, Kutryk MJ, Krenning EP, Roelandt JR, Serruys PW. Site-specific intracoronary heparin delivery in humans after balloon angioplasty. A radioisotopic assessment of regional pharmacokinetics. *Circulation.* 1997;96:154-65.

9. Desai MP, Labhasetwar V, Walter E, Levy RJ, Amidon GL. The mechanism of uptake of biodegradable microparticles in Caco-2 cells is size dependent. *Pharm Res.* 1997;14:1568-73.

10. Cebrián V, Martín-Saavedra F, Yagüe C, Arruebo M, Santamaría J, Vilaboa N. Size-dependent transfection efficiency of PEI-coated gold nanoparticles. *Acta Biomater.* 2011;7:3645-55.

11. Aoki J, Ong AT, Abizaid A, den Heijer P, Bonnier H, McClean DR, Verheye S, Belardi J, Condado JA, Pieper M, Sousa JE, Bressers M, Symons J, Litvack F, Sianos G, Serruys PW. One-year clinical outcome of various doses and pharmacokinetic release formulations of paclitaxel eluted from an erodable polymer - Insight in the Paclitaxel In-Stent Controlled Elution Study (PISCES). *EuroIntervention.* 2005;1:165-72.

12. Davda J, Labhasetwar V. Characterization of nanoparticle uptake by endothelial cells. *Int J Pharm.* 2002;233:51-9.

13. Rogers WJ, Basu P. Factors regulating macrophage endocytosis of nanoparticles: implications for targeted magnetic resonance plaque imaging. *Atherosclerosis.* 2005;178:67-73.

14. Labhasetwar V, Song C, Humphrey W, Shebuski R, Levy RJ. Arterial uptake of biodegradable nanoparticles: effect of surface modifications. *J Pharm Sci.* 1998;87:1229-34.

15. Song C, Labhasetwar V, Cui X, Underwood T, Levy RJ. Arterial uptake of biodegradable nanoparticles for intravascular local drug delivery: results with an acute dog model. *J Control Release.* 1998;54:201-11.

16. Westedt U, Barbu-Tudoran L, Schaper AK, Kalinowski M, Alfke H, Kissel T. Effects of different application parameters on penetration characteristics and arterial vessel wall integrity after local nanoparticle delivery using a porous balloon catheter. *Eur J Pharm Biopharm.* 2004;58:161-8.

17. Finn AV, Kolodgie FD, Harnek J, Guerrero LJ, Acampado E, Tefera K, Skorija K, Weber DK, Gold HK, Virmani R. Differential response of delayed healing and persistent inflammation at sites of overlapping sirolimus- or paclitaxel-eluting stents. *Circulation.* 2005;112:270-8.

18. Schwartz RS, Edelman ER, Carter A, Chronos N, Rogers C, Robinson KA, Waksman R, Weinberger J, Wilensky RL, Jensen DN, Zuckerman BD, Virmani R; Consensus Committee. Drug-eluting stents in preclinical studies: recommended evaluation from a consensus group. *Circulation.* 2002;106:1867-73.

19. Schwartz RS, Chronos NA, Virmani R. Preclinical restenosis models and drug-eluting stents: still important, still much to learn. *J Am Coll Cardiol.* 2004;44:1373-85.

20. Gunn J, Arnold N, Chan KH, Shepherd L, Cumberland DC, Crossman DC. Coronary artery stretch versus deep injury in the development of in-stent neointima. *Heart.* 2002;88:401-5.

21. Schwartz RS, Edelman E, Virmani R, Carter A, Granada JF, Kaluza GL, Chronos NA, Robinson KA, Waksman R, Weinberger J, Wilson GJ, Wilensky RL. Drug-eluting stents in preclinical studies: updated consensus recommendations for preclinical evaluation. *Circ Cardiovasc Interv.* 2008;1:143-53.